Published in final edited form as:
Immunity. 2010 October 29; 33(4): 620–631. doi:10.1016/j.immuni.2010.10.009.

Carcinoembryonic antigen-related cell adhesion molecule-1 regulates granulopoiesis by inhibition of granulocyte-colony stimulating factor receptor

Hao Pan[1,2] and **John E. Shively**[2]

[1]City of Hope Irell & Manella Graduate School of Biological Sciences, Beckman Research Institute of City of Hope, 1450 E. Duarte Rd, Duarte CA 91010, USA

[2]Department of Immunology, Beckman Research Institute of City of Hope, 1450 E. Duarte Rd, Duarte CA 91010, USA

Summary

Although carcinoembryonic antigen-related cell adhesion moclecule-1 (CEACAM1) is an activation marker for neutrophils and delays neutrophil apoptosis, the role of CEACAM1 in granulopoiesis and neutrophil dependent host immune responses has not been investigated. CEACAM1 expression correlated with granulocytic differentiation, and *Ceacam1*$^{-/-}$ mice developed neutrophilia due to loss of the Src- homology-phosphatase-1 (SHP-1) dependent inhibition of granulocyte-colony stimulating factor receptor (G-CSFR)-signal transducer and activator of transcription (Stat3) pathway provided by CEACAM1. Moreover, *Ceacam1*$^{-/-}$ mice were hypersensitive to *Listeria Monocytogenes* (LM) infection with an accelerated mortality. Reintroduction of CEACAM1 into *Ceacam1*$^{-/-}$ bone marrow restored normal granulopoiesis and host sensitivity to LM infection, while mutation of its immunoreceptor tyrosine-based inhibitory motifs (ITIMs) abrogated this restoration. shRNA mediated reduction of Stat3 amounts rescued normal granulopoiesis attenuating host sensitivity to LM infection in *Ceacam1*$^{-/-}$ mice. Thus, CEACAM1 acted as a co-inhibitory receptor for G-CSFR regulating granulopoiesis and host innate immune response to bacterial infections.

Introduction

Neutrophils, the largest subset of granulocytes, are the first line of defense against various infections caused by bacteria, fungi and parasites. Neutrophils traffic into infected tissues and clear pathogens, while secreting pro-inflammatory cytokines that may cause tissue damage (Nathan, 2006). Due to their short life span, hematopoietic stem cells continuously produce granulocytes at a basal or emergent stage requiring a strict regulation of granulopoiesis (Christopher and Link, 2007).

Granulocyte-colony stimulating factor receptor (G-CSFR) is the master regulator of granulopoiesis since both G-CSF and G-CSFR genetically ablated mice develop severe

Correspondence should be addressed to: J.E. Shively, JShively@coh.org.

Author contributions: H.P. designed and performed research, analyzed data, and wrote the manuscript; J.E.S. supervised research and revised the manuscript.

neutropenia (Lieschke et al., 1994; Liu et al., 1996). Binding of G-CSF to G-CSFR activates a signaling cascade including phosphorylation of signal transducer and activator of transcription (Stat3) a key regulator of basal and emergent granulopoiesis (Avalos, 1996). Similar with its function as a pro-proliferative oncogene in tumor (Yu et al., 2009), Stat3 also promotes mitogenic signaling to facilitate neutrophil production in response to G-CSF (Avalos, 1996), and hyper-active Stat3 induces enhanced granulopoiesis (Croker et al., 2004). Consistent with the finding that Stat3 antagonizes Stat1 and Stat5 activation in T helper cell differentiation and tumor environment (Welte et al., 2003) G-SCF only weakly activates Stat1 and Stat5 in Stat3 proficient models (Avalos, 1996; Chakraborty et al., 1996; Tian et al., 1994). However, once the antagonizing function of Stat3 is lost in Stat3 conditional genetically ablated mice, hyper-active Stat1 compensates for Stat3 and becomes an alternative G-CSFR downstream pathway, resulting in neutrophilia (Lee et al., 2002). Taken together, Stat3 expression and activation need to be properly controlled for normal granulopoiesis. In addition, loss of β_2-integrin or leukocyte-endothelial (LE)-selectin induces neutrophilia due to elevated basal amounts of G-CSF and IL-17 (Forlow et al., 2001; Stark et al., 2005), suggesting a non-cellular autonomous feedback mechanism, while loss of CXC-chemokine receptor-4 (CXCR-4) affects granulopoiesis in a cellular autonomous fashion (Eash et al., 2009). The possibility that inhibitory co-receptors may also regulate G-CSFR dependent granulopoiesis has not been investigated.

In this respect, CEACAM1 is a likely candidate based on its high expression on neutrophils and its known role as an inhibitory co-receptor in the immune system (Gray-Owen and Blumberg, 2006). The CEACAM1 molecule consists of cytoplasmic, transmembrane and extracellular domains. The extracellular domains comprise a membrane distal IgV- like N-domain followed by a variable number of IgC-like domains. The N-domain mediates homophilic ligation with other CEACAM1 molecules or heterophilic ligation with other CEA family members (Gray-Owen and Blumberg, 2006). Both human and murine CEACAM1 transcripts undergo alternative splicing generating 11 human and 4 murine isoforms (Gray-Owen and Blumberg, 2006).

The CEACAM1 long form has two ITIMs in its cytoplasmic domain, which upon phosphorylation recruit Src homology domain–containing protein-tyrosine phosphatases SHP-1 and -2, which in turn, suppress signal transduction of associated receptors by de-phosphorylation of their downstream effectors (Gray-Owen and Blumberg, 2006). In activated T cells, recruitment of SHP-1 by CEACAM1 down-regulates TCR signaling by targeting Zap-7 (Chen et al., 2008) and IL-2R signaling (Chen and Shively, 2004). Over-expression of CEACAM1 long forms in T-cells prevents inflammatory bowel disease (IBD) in a murine colitis model (Nagaishi et al., 2006). In germinal B cells, anti-IgM induces CEACAM1 phosphorylation, SHP-1 recruitment, and subsequent suppression of PI3-K signaling, leading to potentiated activation induced cell death (AICD) (Lobo et al., 2009). Although these studies demonstrate how CEACAM1 regulates immune effector cell function, the possibility that CEACAM1 may regulate immune cell development has not been addressed. Although CEACAM1 plays a role in activation and apoptosis of neutrophils (Singer et al., 2005; Singer et al., 2002), its role in granulopoiesis and neutrophil dependent innate immune response in infectious models has not been investigated.

Here, we use retroviral transduction and bone marrow reconstitution to reintroduce CEACAM1, ITIM mutated CEACAM1 into *Ceacam1*$^{-/-}$ bone marrow (BM), or to normalize p-Stat3 amounts in *Ceacam1*$^{-/-}$ BM and study the effects on granulopoiesis and innate immune response. Our results demonstrate that CEACAM1 regulates myeloid development by functioning as a co-inhibitory receptor of G-CSFR through ITIM and SHP-1, leading to down-regulation of downstream Stat3 activation, and the absence of

CEACAM1 results in elevated G-CSFR-Stat3 signaling and neutrophilia, which in turn, adversely affects the innate immune response to pathogenic bacteria.

Results

CEACAM1 is a granulocytic lineage differentiation marker

Neutrophils, monocytes, and macrophages from wild type (WT) mice expressed high amounts of CEACAM1, with neutrophil expression found at a significantly higher amount compared to monocytes and macrophages (Figure 1A). In addition, peripheral blood neutrophils (PBNs) that are more mature than bone marrow neutrophils (BMNs), expressed a slightly higher amount of CEACAM1 on the cell surface than BMNs. We also examined the expression of CEACAM1 on lineage negative bone marrow (Lin^- BM) cells by immunoblot (Figure 1B) and flow cytometric analysis (Figure 1C). Although these progenitor cells expressed a relatively lower amount of CEACAM1 compared to the mature innate immune cells, granulocyte-monocyte progenitors (GMPs) that specifically give rise to granulocytes and monocytes, expressed higher amounts of CEACAM1 than common myeloid precursors (CMPs) and megakaryocyte-erythrocyte precursors (MEPs) (Figure 1C). These results indicate that from the early progenitor stage to the final effector stage, cell surface CEACAM1 amounts correlate with granulocytic lineage differentiation. We also compared the long and short forms of CEACAM1 by quantitative real-time PCR using CEACAM1 long form and short form specific primers showing that neutrophils and Lin^- BM cells expressed both the long and short forms of CEACAM1 at the mRNA level (Figure 1D) with a general preference for the long form (in neutrophils, the Long:Short (L:S) ratio was about 1.76; in Lin^- BM cells, the L:S ratio was about 1.41).

Genetic ablation of CEACAM1 leads to dysregulated granulopoiesis due to neutrophil progenitor cell hyper-proliferation

Since CEACAM1 is expressed on neutrophil progenitors (Figure 1 B-D) and is a known inhibitory co-receptor on activated lymphocytes (Gray-Owen and Blumberg, 2006), we hypothesized that granulocytic development and production would be affected in *Ceacam1*$^{-/-}$ mice. In contrast to WT C57BL/6 mice, *Ceacam1*$^{-/-}$ mice spontaneously developed systemic neutrophilia as manifested by the dramatically higher numbers of the Ly-6G$^+$CD11b$^+$ population in BM, peripheral blood (PB), spleen and liver (Figure 2A). This dysregulated granulopoiesis could be explained by an accumulation of neutrophils with a slower turnover rate or an augmented neutrophil production from myeloid progenitor cells. To test the first possibility, we utilized the in vitro spontaneous apoptosis assay (Johnnidis et al., 2008) and found that *Ceacam1*$^{-/-}$ neutrophils underwent normal or slightly faster apoptosis than WT ones (Figure S2A-B). To test the second possibility, we assessed neutrophil progenitor cell proliferation in the methylcellulose colony formation assay. G-CSF treated *Ceacam1*$^{-/-}$ BM produced 2-fold more neutrophil colonies than WT (Figure 2B). *Ceacam1*$^{-/-}$ BM had 1.6 times the number of GMPs than WT (Figure 2C). When the proliferative capacity of the GMPs was measured by bromodeoxyuridine (BrdU) incorporation, there was a higher ratio of BrdU$^+$ GMPs in *Ceacam1*$^{-/-}$ mice than the WT (Figure 2D). Since there was no obvious difference in BrdU incorporation of WT or *Ceacam1*$^{-/-}$ neutrophils (data not shown), the observed neutrophilia in *Ceacam1*$^{-/-}$ mice does not result from proliferation of neutrophils. In G-CSF induced emergent granulopoiesis (Croker et al., 2004; Roberts et al., 1997) in WT mice, bone marrow neutrophil and peripheral blood counts were 21×10^6 and 15×10^5/ml, respectively, while in G-CSF treated *Ceacam1*$^{-/-}$ mice enhanced granulopoiesis was observed (BMN 95×10^6, PBN 112×10^5/ml) (Figure 2E). These results suggest that CEACAM1 negatively regulates G-CSF mediated basal (homeostatic) and emergent granulopoiesis, and that genetically ablating CEACAM1 leads to neutrophilia due to neutrophil progenitor cell hyper-proliferation.

Ceacam1$^{-/-}$ BM cells act autonomously and CEACAM1 regulation of progenitor cells is granulocytic lineage-specific

β_2-integrin or LE-selectin genetically ablated mice develop neutrophilia in a non-autonomous feedback mechanism (Forlow et al., 2001; Stark et al., 2005). To study is this mechanism aplies to CEACAM1, reverse BM reconstitution was performed in which we transplanted WT BM cells into lethally irradiated *Ceacam1*$^{-/-}$ recipients or *Ceacam1*$^{-/-}$ BM cells into lethally irradiated WT recipients. *Ceacam1*$^{-/-}$ BM cells act independently since WT recipients receiving *Ceacam1*$^{-/-}$ BM cells developed neutrophilia while *Ceacam1*$^{-/-}$ recipients that received WT BM cells did not (Figure S2C).

To test if CEACAM1's regulation on progenitor cells is granulocytic lineage specific, we carried out a BM competition assay in which equivalent amounts of BM cells from *Ceacam1*$^{-/-}$ C57BL/6 (CD45.2) and congenic WT C57BL/6 (CD45.1) mice were co-injected into lethally irradiated WT C57BL/6 recipients. We found that 81% of the BMNs expressed CD45.2, while for BM B cells, the ratio of CD45.1$^+$: CD45.2$^+$ was close to 1:1 (Figure S2D), a result consistent with our observation that *Ceacam1*$^{-/-}$ mice did not have abnormal numbers of BM or spleen B- or T- cells (data not shown). We also found that there were more CD45.2$^+$ (*Ceacam1*$^{-/-}$ BM derived) GMP populations than CD45.1$^+$, confirming CEACAM1 regulates early granulopoiesis autonomously (data not shown). In methylcellulose assays, *Ceacam1*$^{-/-}$ and WT BM gave rise to similar numbers of erythrocyte, megakaryocyte or macrophage colonies (Figure S3E). We conclude that the effect of CEACAM1 on progenitor cells is granulocytic lineage-specific.

CEACAM1 down-regulates G-CSFR Stat3 signaling

Since CEACAM1 acts as a co-inhibitory receptor for many receptors (Gray-Owen and Blumberg, 2006) and G-CSFR is the central mediator of granulopoiesis (Avalos, 1996), we hypothesized that CEACAM1 negatively regulates G-CSFR signaling. Treatment of WT Lin$^-$ BM cells with G-CSF induced significant tyrosine phosphorylation of CEACAM1, while IP of CEACAM1 co-IPed G-CSFR in the G-CSF treated Lin$^-$ BM cells indicating that CEACAM1 is physically associated with G-CSFR after G-CSF treatment (Figure 3A). Accordingly, the amount of p-Stat3 in *Ceacam1*$^{-/-}$ Lin$^-$ BM cells was 2-fold higher than in the WT Lin$^-$ BM cells after G-CSF treatment (Figure 3B), as well as increased amounts of p-Stat3 in *Ceacam1*$^{-/-}$ GMPs as measured by intra-cellular staining (Figure 3C). Analysis of other G-CSFR downstream molecules exhibited no difference of p-Stat1, p-Stat5, p-Akt or p-Erk1/2 between WT and *Ceacam1*$^{-/-}$ Lin$^-$ BM cells after G-CSF treatment (Figure S3). The pro-proliferative Stat3 target genes, CyclinD1 and C-Myc, (Yu et al., 2009), were induced at a higher amount in Lin$^-$ BM cells after G-CSF treatment (Figure 3D). Also, sorted *Ceacam1*$^{-/-}$ GMPs transcribed more CyclinD1 and C-Myc mRNA after G-CSF treatment (Figure 3E). Thus, elevated Stat3 activation is primarily responsible for neutrophilia in *Ceacam1*$^{-/-}$ mice.

CEACAM1 inhibits G-CSFR-Stat3 signaling and granulopoiesis through ITIM recruitment of SHP-1

The CEACAM1 long form contains two ITIMs and is the isoform that mediates a SHP-1 dependent suppressive signal upon ITIM phosphorylation (Gray-Owen and Blumberg, 2006). Although WT Lin$^-$ BM cells expressed both long and short isoform transcripts of CEACAM1, we assumed that the inhibitory effect of CEACAM1 on granulopoiesis and G-CSFR signaling is ITIM-SHP-1 dependent. To test this hypothesis, we reintroduced CEACAM1 long form (CEACAM1-2L, CEACAM1-4L), short form (CEACAM1-2S, CEACAM1-4S) and ITIM tyrosine mutated long form (CEACAM1-2Lm and CEACAM1-4Lm) into *Ceacam1*$^{-/-}$ BM stem cells, and transplanted them into lethally irradiated *Ceacam1*$^{-/-}$ recipients (Figure S4A-C). Two months after reconstitution, we

found that CEACAM1 long forms, but not the short forms, restored normal neutrophil populations (Figure 4A-B), normal GMP populations (data not shown), and normal p-Stat3 amounts (Figure 4C). Moreover mutating the tyrosines in the ITIMs prevented this restoration (Figure 4A-C).

We carried out IP analysis to determine if the physical interaction between CEACAM1 and G-CSFR is ITIM-SHP-1 dependent. Interestingly, G-CSF induced tyrosine phosphorylation of both the CEACAM1 long form and short form (the murine CEACAM1 short forms have a tyrosine site in their cytoplasmic domains) (Figure 4D). As expected, there was no tyrosine phosphorylation of CEACAM1 in the Lin^- BM cells isolated from *Ceacam1*$^{-/-}$ mice reintroduced with CEACAM1-2Lm, CEACAM1-4Lm or empty vector (Figure 4D). Consistent with our hypothesis, G-CSFR was pulled down by anti-CEACAM1 upon G-CSF treatment only in the Lin^- BM cell lysates isolated from *Ceacam1*$^{-/-}$ mice reintroduced with CEACAM1 long form (Figure 4D). We also demonstrated that CEACAM1 associates with SHP-1 upon G-CSF treatment in WT Lin^- BM cells (Figure 3A), or Lin^- BM cells isolated from *Ceacam1*$^{-/-}$ mice receiving CEACAM1-2L or CEACAM1-4L (Figure 4D), but not in Lin^- BM cells recovered from *Ceacam1*$^{-/-}$ mice receiving CEACAM1-2S, 4S, CEACM1-2Lm, 4Lm, or empty vector (Figure 4D). Thus, CEACAM1-SHP-1 association depends on the presence of the ITIMs in CEACAM1 long forms. In WT Lin^- BM cells, SHP-1 also directly associated with G-CSFR as shown by IPs using anti-SHP-1 antibody (Figure 4E), leading to dephosphorylation of G-CSFR (Figure 4F). Notably, the SHP-1-G-CSFR association was abrogated in *Ceacam1*$^{-/-}$ Lin^- BM cells, revealing the indispensable role of CEACAM1 in recruiting SHP-1 to dephosphorylate G-SCFR. Lastly, the dependency of SHP-1 was confirmed by shRNA-mediated reduction of SHP-1 in WT mice, a treatment that caused augmented granulopoiesis associated with elevated G-CSFR-Stat3 signaling (Figure S4D-G). Therefore, we conclude that the CEACAM1 down-regulation of the G-CSFR-Stat3 pathway depends on its ITIMs and recruitment of SHP-1.

Modulation of CEACAM1 regulates host immune response to LM infection

To study the physiological impact of the enhanced granulopoiesis of *Ceacam1*$^{-/-}$ mice, they were infected with *Listeria Monocytogenes* (LM), an infectious model in which neutrophils play an indispensable role in clearance during the early stages of infection (Eash et al., 2009; Nathan, 2006; Zhu et al., 2009). Although enhanced bacteria clearance and prolonged survival of *Ceacam1*$^{-/-}$ mice due to their neutrophilia was a likely outcome, it is also possible that loss of negative signaling by CEACAM1 and neutrophilia could lead to enhanced tissue damage and pro-inflammatory cytokine production. Indeed, *Ceacam1*$^{-/-}$ mice died dramatically faster than the WT mice; in fact, almost all *Ceacam1*$^{-/-}$ mice died within 7 days while the WT mice had a 40% survival rate even at day 12 (Figure 5A). Bacterial colonies in either the liver or spleen of *Ceacam1*$^{-/-}$ mice 3 days post infection were fewer compared with WT, showing that *Ceacam1*$^{-/-}$ mice had improved bacterial clearance (Figure 5B). Therefore, the accelerated mortality was probably not due to failure of bacterial clearance in *Ceacam1*$^{-/-}$ mice. Since it was also possible that lack of CEACAM1 affects neutrophil anti-bacterial functions, an in vitro bacterial killing assay was performed. In this assay there was no significant difference between *Ceacam1*$^{-/-}$ and WT neutrophils (Figure S5A). Importantly, *Ceacam1*$^{-/-}$ neutrophils also performed normally in actin-cytoskeleton rearrangement and migration assays (Figure S5B-C). Therefore, the improved bacterial clearance in *Ceacam1*$^{-/-}$ mice was not due to abnormal migration or an abnormal bacterial killing function of *Ceacam1*$^{-/-}$ neutrophils, but instead was due to increased neutrophil numbers in *Ceacam1*$^{-/-}$ mice. However, the improved bacterial clearance in infected *Ceacam1*$^{-/-}$ mice was accompanied by severe tissue damage and necrosis in the liver (Figure 5C**, quantified in** Figure S5D), likely caused by neutrophils. Indeed, significantly more neutrophils were recovered in infected *Ceacam1*$^{-/-}$ livers than in

the WT ones (Figure 5D). In addition, in LM infected *Ceacam1*$^{-/-}$ mice, serum amounts of interleukin-1β (IL-1β), which was in the range associated with endotoxic shock (Greten et al., 2007), and IL-6, keratinocyte-derived chemokine (KC), tumor necrosis factor-α (TNF-α) to a lesser degree, were higher compared to WT mice (Figure 5E).

To further elucidate the cause of the elevated pro-inflammatory cytokine amounts in vivo, we analyzed whether CEACAM1 regulates cytokine production on a cellular basis. We examined neutrophils and macrophages, two major cellular sources of cytokine production during early days post infection. When cells were stimulated in vitro with lipopolysaccharide (LPS), a toll-like receptor 4 (TLR4) ligand, or peptidoglycan (PGN), a TLR2 ligand, no significant difference in IL-1β, TNF-α, IL-6 and KC production was observed between WT and *Ceacam1*$^{-/-}$ macrophages (Figure S6A). Interestingly, *Ceacam1*$^{-/-}$ neutrophils produced significantly more IL-1β (manuscript in preparation) but similar amount of TNF-α, IL-6 and KC compared with WT neutrophils (Figure S6B). We conclude that while loss of CEACAM1 significantly affects neutrophil IL-1β production, there was no obvious effect on the production of other pro-inflammatory cytokines. Also, loss of CEACAM1 does not seem to affect macrophage production of pro-inflammatory cytokines. Based on the in vitro per cell based cytokine production profile, we inferred that the significantly higher serum amount of IL-1β in *Ceacam1*$^{-/-}$ mice after LM infection was due to both elevated neutrophils and elevated IL-1β production capacity by individual *Ceacam1*$^{-/-}$ neutrophils, while the moderately higher amounts of TNF-α, IL-6 and KC were likely due to increased neutrophil numbers only in *Ceacam1*$^{-/-}$ mice.

Since neutrophilia in WT mice can be induced by G-CSF treatment (Croker et al., 2004; Roberts et al., 1997), it was possible to examine the effects of increased neutrophils on cytokine production during LM infection. Indeed, in response to LM infection, the G-CSF treated WT mice, which have comparable numbers of bone marrow and peripheral blood neutrophils as the *Ceacam1*$^{-/-}$ mice without G-CSF treatment (Figure 2E), exhibited similar serum amounts of TNF-α, IL-6 and KC as *Ceacam1*$^{-/-}$ mice (Figure S6C) and had a similar degree of liver damage (Figure S6D**, quantified in** Figure S6E), both of which were probably due to the abnormal number of neutrophils. However, their serum amount of IL-1β was dramatically lower than in *Ceacam1*$^{-/-}$ mice, and the G-CSF treated WT mice showed better survival than *Ceacam1*$^{-/-}$ mice (Figure S6F). Although the G-CSF treated WT mice had better bacterial clearance than untreated WT mice (data not shown), they showed poorer survival than the WT mice (Figure S6F), which could be due to the liver damage and elevated cytokine amounts as shown above, consistent with previous studies showing G-CSF treatment potentiated neutrophil induced tissue damage and pro-inflammatory response (Croker et al., 2004; Roberts et al., 1997).

These results also indicated that the hypersensitivity of *Ceacam1*$^{-/-}$ mice to LM infection was not solely due to the increased number of neutrophils, but was partially due to elevated pro-inflammatory cytokine amounts, especially IL-1β. Based on these findings, we conclude that the combination of severe liver damage and high pro-inflammatory cytokine amounts induced accelerated mortality of LM infected *Ceacam1*$^{-/-}$ mice.

We also studied LM infected *Ceacam1*$^{-/-}$ mice reconstituted with CEACAM1-2L, CEACAM1-4L CEACAM1-2S, CEACAM-4S, CEACAM1-2Lm, CEACAM1-4Lm or empty vector transduced *Ceacam1*$^{-/-}$ BM cells. As expected, only CEACAM1-2L or CEACAM1-4L rescued *Ceacam1*$^{-/-}$ mice from hypersensitivity to LM infection (Figure 6A) with manifestation of greatly less liver damage (Figure 6B**, quantified in** Figure S6G) and lower serum cytokine amounts (Figure 6C).

Reduction of Stat3 with shRNA restores normal granulopoiesis and attenuates host sensitivity to LM infection of *Ceacam1*$^{-/-}$ mice

To confirm that elevated G-CSFR-Stat3 signaling was responsible for enhanced granulopoiesis and the corresponding hypersensitivity to LM infection of *Ceacam1*$^{-/-}$ mice, we reduced Stat3 amounts with Stat3 shRNA in *Ceacam1*$^{-/-}$ BM cells followed by re-injection into lethally irradiated *Ceacam1*$^{-/-}$ mice. Two months after BM reconstitution we found that reduction of Stat3 amounts by shRNA completely restored normal granulopoiesis both in vivo and in vitro (Figure 7A-B**)** as well as normal GMP amounts (data not shown). Immunoblot analysis showed that the reduction of total Stat3 in *Ceacam1*$^{-/-}$ Lin^{-} BM cells by shRNA was around 65%, which in turn, reduced p-Stat3, C-Myc, CyclinD1 to the WT amounts after G-CSF stimulation (Figure 7C). In contrast, Stat1 and Stat5 remained weakly phosphorylated after reduction of total Stat3, confirming that Stat3 plays a dominant role downstream of G-CSFR. shRNA specificity was confirmed since shStat3 did not affect Stat1 or Stat5 amounts, and the shRNA control did not affect Stat protein amounts, ruling out the possibility of off-target effects. We then challenged these mice with LM and examined if normalized granulopoiesis could rescue the accelerated mortality of *Ceacam1*$^{-/-}$ mice. Indeed, reduction of Stat3 partially rescued *Ceacam1*$^{-/-}$ mice from hypersensitivity to LM infection as manifested by prolonged survival (Figure 7D) associated with less liver damage (Figure 7E**, quantified in** Figure S7) and lower serum amounts of IL-6, TNF-α, and KC (Figure 7F). However, IL-1β remained high after reduction of total Stat3 by shRNA (Figure 7F), a finding that might explain their relatively poorer survival compared with WT mice, especially at early days post infection.

Discussion

Although CEACAM1 has been designated as a marker for neutrophil activation (Singer et al., 2002) and plays a role in neutrophil apoptosis (Singer et al., 2005), a role for CEACAM1 in granuolopoiesis has not been studied. Here, we showed CEACAM1 is a granulocytic lineage differentiation marker, and *Ceacam1*$^{-/-}$ mice had severe neutrophilia associated with hyper-proliferation of *Ceacam1*$^{-/-}$ neutrophil progenitor cells. This finding, together with the general function of CEACAM1 as an inhibitory co-receptor in T-cells (Gray-Owen and Blumberg, 2006), led us to hypothesize that CEACAM1 may down-regulate neutrophil production by acting as a co-inhibitory receptor for G-CSFR, the master regulator of granulopoiesis (Liu et al., 1996; McLemore et al., 2001). This hypothesis was strengthened by the finding that in Lin^{-} BM cells G-CSFR was co-IPed with CEACAM1 when treated with G-CSF, and that under this condition CEACAM1 was phosphorylated on its ITIMs and recruited SHP-1. The recruitment of SHP-1 down-regulated G-CSFR signaling by decreasing the phosphorylation of G-CSFR, attenuating its downstream Stat3 activation and expression of mitogenic proteins Cyclin D1 and C-Myc, thereby controlling the proliferation of neutrophil progenitors. In the absence of CEACAM1 the negative feedback loop would be absent allowing neutrophil precursors to abnormally produce neutrophils.

The inhibitory activity of CEACAM1 resides in the long isoforms that have two ITIMs that when phosphorylated recruit SHP-1 and -2 (Gray-Owen and Blumberg, 2006). Using retroviral vector transduced BM stem cell based BM reconstitution assays, we demonstrated that the CEACAM1 long form was able to associate with G-CSFR and restore normal granulopoiesis and that mutation of the tyrosine residues in its ITIMs abrogated this restoration. Furthermore, we found that only the CEACAM1 long forms recruited the suppressive phosphatase SHP-1, and that SHP-1 antibodies were able to co-IP G-CSFR, leading to de-phosphorylation of activated G-CSFR. We demonstrated the dependency of SHP-1 in regulating granulopoiesis by reduction of SHP-1 in WT mice by shRNA, a treatment which also leads to enhanced G-CSFR-Stat3 signaling and granulopoiesis,

consistent with the previous observation that SHP-1 genetically ablated mice develop neutrophilia (Kruger et al., 2000). Interestingly, G-CSF also induced tyrosine phosphorylation of the short isoform, although this isoform did not appear to associate with SHP-1 or regulate granulopoiesis. This intriguing result leaves open a role for the tyrosine residue in the murine short form of CEACAM1, although it is not present in the context of an ITIM. Notably, the human CEACAM1 short isoform has phenylalanine in place of tyrosine (Chen et al., 2007). Thus, further studies are required to determine if the short isoform in murine CEACAM1 has any additional functions upon phosphorylation of its tyrosine residue.

Stat3, an oncogene in many tumors (Yu et al., 2009), is the dominant Stat protein downstream of G-CSFR that positively regulates granulopoiesis (Avalos, 1996). Stat3 also regulates proliferation of early progenitor cells of granulocytes (Zhang et al.) and is subject to negative regulation by induction of SOCS3, a negative feedback loop of Stat signaling (Croker et al., 2004). As expected, *Socs3*$^{-/-}$ mice have hyper-p-Stat3 and enhanced granulopoiesis (Croker et al., 2004). Similarly, our study of *Ceacam1*$^{-/-}$ mice serves as another example in which loss of a negative regulator leads to hyper-p-Stat3 and hyper-granulopoiesis. We examined this further by reducing Stat3 amounts in *Ceacam1*$^{-/-}$ mice, which in turn, normalized p-Stat3 amounts and completely restored normal granulopoiesis, confirming that hyper-p-Stat3 was the main factor responsible for neutrophilia in *Ceacam1*$^{-/-}$ mice. Notably, Stat3 also antagonizes Stat1 and Stat5 activation (Lee et al., 2002), which explains the weak activation of Stat1 and Stat5 in response to G-CSF in Stat3 proficient models (Avalos, 1996; Chakraborty et al., 1996; Tian et al., 1994), while loss of Stat3 leads to alternative Stat1 hyper-activation, which in turn, compensates for Stat3 and causes neutrophilia (Lee et al., 2002). Although these investigators interpret these results as evidence that Stat3 is a negative regulator of granulopoiesis, we argue that loss of Stat3 abrogates its normal antagonistic function on Stat1 and Stat5 signaling.

Similar antagonizing mechanisms occur in T helper (Th) cell differentiation and activation, where loss of Stat3 leads to augmented Stat1 activation and Th1 cell response (Welte et al., 2003). In the case of the Stat3 conditional gene ablated studies (Lee et al., 2002), evidence is provided that Stat3 is a negative regulator of Stat1 and Stat5 in granulopoiesis, but no evidence is provided that Stat3 is a negative regulator of granulopoiesis in wild type or any other Stat3 proficient mice.

In this regard, Stat3 proficient *Socs3*$^{-/-}$ mice (Croker et al., 2004), is not the equivalent situation to the Stat3 conditionally ablated mouse model, in which Stat1 mediated enhanced granulopoiesis (Lee et al., 2002). Although the study of the *Socs3*$^{-/-}$ mice shows the crucial nature of the negative feedback loop provided by the Stat3 target gene SOCS3, it does not disregard Stat3's major function of transcribing mitogenic factors that positively regulate granulopoiesis. Instead, there is an exaggerated outcome demonstrating Stat3's role as a positive regulator in the absence of negative regulation. Take together, we can reconcile these previous studies and summarize Stat3's function in G-CSF mediated granulopoiesis as follows: Stat3 is the dominant Stat protein downstream of G-CSFR, and when present, it positively regulates granulopoiesis by promoting mitogenic signaling. One the one hand, Stat3 is subject to negative regulatory mechanisms including its self-induction of SOCS3, and that loss of the inhibitory mechanism(s) leads to hyper Stat3 activation, augmented mitogenic signaling and enhanced granulopoiesis. But on the other hand, Stat3 antagonizes or negatively regulates Stat1 and Stat5 activation, and when Stat3 is totally absent, its antagonizing role is lost and Stat1 becomes hyper active, a result that not only compensates for loss of Stat3 but also leads to neutrophilia. With this in mind, we gain a fuller appreciation that Stat3 expression and activation must be properly controlled for normal granulopoiesis.

The absence of CEACAM1 in the *Ceacam1*$^{-/-}$ mice not only led to neutrophilia, but also caused a major problem in their in vivo response to LM infection. Although the surplus of neutrophils caused enhanced bacteria clearance in the *Ceacam1*$^{-/-}$ mice, they also induced severe liver damage and elevated serum cytokine amounts, especially IL-1β, leading to accelerated mortality, especially during the early days in which innate immunity predominates. Whether there are strain (C57B/6) effects on G-CSF treatment and LM infection experiment could be tested in the future when *Ceacam1*$^{-/-}$ mice on other backgrounds are available. Interestingly, reintroduction of CEACAM1 long form but not the short form or ITIM mutated long form to *Ceacam1*$^{-/-}$ mice not only restored normal granulopoiesis, but also normalized amounts of IL-1β, which correspondingly completely restored normal sensitivity to LM infection, demonstrating a critical checkpoint function for CEACAM1. However, it is worth noting that this checkpoint role is not limited to the G-CSFR-Stat3 pathway of granulopoiesis, since while reduction of total Stat3 amounts in *Ceacam1*$^{-/-}$ BM by shRNA completely restored normal granulopoiesis, serum IL-1β amounts remained high. We also examined whether loss of CEACAM1 affects cellular cytokine production by stimulating neutrophils and macrophages in vitro. Although no obvious difference in the cytokine production between WT and *Ceacam1*$^{-/-}$ macrophages was observed, *Ceacam1*$^{-/-}$ neutrophils produced slightly more IL-6, and significantly more IL-1β production (manuscript in preparation). Why loss of CEACAM1 preferably affects cytokine (IL-1β) production in neutrophils but not in macrophages remains an open question. Thus, our studies reveal CEACAM1 regulates both the quantitative and qualitative response of neutrophils to infection.

In summary, CEACAM1 provides a critical negative feedback loop in the regulation of granulopoiesis and the corresponding innate immune response to infections, demonstrating the “fine tuning” of the innate immune system by a co-inhibitory receptor. These insights should help us better understand the interactions between cell surface receptors orchestrating innate immune system development, and may have clinical implications in treating infectious, auto-inflammatory and other innate immunity related diseases.

Methods

Mice strains

Ceacam1$^{-/-}$ mice (C57B/6 background) were generated by Beauchemin and coworkers (Hemmila et al., 2004). C57BL/6 mice were from National Cancer Institute and congenic CD45.1 C57B/6 mice were from The Jackson Laboratory. 7-12 weeks old mice were used for all the experiments. To induce emergent granulopoiesis, G-CSF (2.5ug/mouse, twice a day) was injected intraperitoneally (i.p.) into mice for 5 consecutive days.

Listeria Monocytogenes infection and colony counting

Listeria Monocytogenes EGD (ATCC) were cultured overnight in DIFCO *Listeria* Enrichment Broth (BD Biosciences). Colony-forming units (CFUs) of LM were determined by plating serial dilutions of LM on BBL CHROMagar *Listeria* plates (BD Biosciences). 2.5×10^5 CFUs of LM were injected i.p. into mice. 24 hours later, peripheral blood was collected for cytokine amounts. 72 hours later, livers and spleens were collected for histology and measurement of bacterial colony numbers 48 hours after plating.

Quantitative Real-time PCR

RNA extractions were performed using Trizol (Invitrogen). Reverse transcription was performed (QIAGEN) by real-time on a Bio-Rad IQ5. CEACAM1 isoforms, Cyclin D1 and C-Myc mRNA expression was normalized to HPRT. Primer sequences will be provided upon request.

Construction and generation of retroviral vectors

CEACAM1-2L, 4L, 2S or 4S cDNAs were cloned into retroviral vector (MSCV-EGFP). The ITIM mutations on CEACAM1-2L and -4L were generated using QuikChange XL Site-Directed Mutagenesis Kit (Stratagene) The shRNA control vector, shStat3 vector (pGFP-V-RS) and Sh SHP-1 vector (pGFP-V-RS) were from Origene, and the target sequence of shStat3 vector is 5′- AGTTCCTGGCACCTTGGATTGAGAGTCAA-3′, and the target sequence of shSHP-1 vector is 5′- TTGTGCGTGAGAGTCTCAGCCAACCTGGT-3′. All retroviral vectors were generated in Phoenix-Eco packaging cell line. For MSCV-EGFP based vectors, viral titers of the supernatants from the stable virus-producing cells were determined in NIH 3T3 cells by flow cytometry. Primer sequences will be provided upon request.

Bone marrow reconstitution assays

For reverse BM reconstitution assays, 7 week old WT or *Ceacam1*$^{-/-}$ mice were lethally irradiated with 1000 Gy, and 5 × 10^6 *Ceacam1*$^{-/-}$ or WT BM cells were intravenously (i.v.) injected into the mice 8 hours after irradiation. 2 months later, mice were sacrificed and the ratio of cell lineages assessed by flow cytometry. For BM competition assays, 7 week old WT mice were co-injected with equivalent (1 × 10^6) *Ceacam1*$^{-/-}$ (CD45.2) and congenic WT (CD45.1) BM cells after lethal irradiation.

Retroviral transduction of bone marrow stems cells

5-Fluorouracil (5 mg/mouse) was injected i.p. into *Ceacam1*$^{-/-}$ mice and BM stem cells were collected 5 days later and expanded in 10% FBS DMEM plus 20 ng/mL IL-3, 50 ng/mL IL-6 and SCF for 24 hours. Viral based empty vector, CEACAM1-2L, 4L, 2S, 4S, 2Lm and 4Lm transduced cells were sorted 48 to 72 hours later as GFP positive cells. Viral expressed shRNA control vector, shStat3 vector and shSHP-1 vector, were selected with puromycin (1 μg/ml) 7 days later. Collected cells were injected i.v into lethally irradiated *Ceacam1*$^{-/-}$ recipients (1-5 × 10^5 cells/mouse) and phenotyped two months later.

Cell sorting and flow cytometric analysis

Lineage negative BM (Lin^- BM) cells were purified using antibody-magnetic bead depletion (Zhu et al., 2009). Neutrophils ($Ly\text{-}6G^+CD11b^+$) were labeled with FITC or PE-Cy5-conjugated anti-Ly-6G, APC-Cy7- conjugated anti-mouse CD11b. Monocytes ($Ly\text{-}6C^+CD11b^+$) were labeled with PE-conjugated anti-mouse Ly-6C, APC-Cy7-conjugated anti-mouse CD11b and macrophages ($Ly\text{-}6C^-CD11b^+F4/80^+$) were labeled with PE-conjugated anti-mouse Ly-6C, APC-Cy7-conjugated anti-mouse CD11b and APC-conjugated F4/80. GMP, CMP and MEP, Lin^- BM cells were labeled with FITC-conjugated anti-CD16-32, APC-conjugated or PE-Cy5 conjugated anti-CD34, PE-Cy7-conjugated anti-Sca-1, PE-conjugated anti-IL-7Rα and APC-Cy7-conjugated anti-C-kit. Cells were permeabilized (BD Cytofix/Cytoperm™) for intracellular staining of p-Stat3 and Stat3 on a FACS Canto II (BD Biosciences).

BrdU incorporation assays

BrdU was injected i.p into mice immediately followed by i.p. injection of LPS (25 μg/kg) or PBS. Six hours later, mice were sacrificed and GMPs were labeled as described above. BrdU was detected with APC-conjugated antibody from BD.

Methylcellulose colony forming assays

5 × 10^4 Lin^- BM cells were cultured in Methylcellulose media supplemented with 20ng/ml G-CSF, 20ng/ml GM-CSF, 10ng/ml SCF, 15ng/ml EPO and 10ng/ml TPO (Sigma). After

incubating at 37 °C 5% CO_2 for 10 days, granulocyte colony numbers were counted according to corresponding morphologies.

Immunoblot, immunoprecipitation and ELISA

Lin^- myeloid progenitors (5×10^6) with or without G-CSF treatment were lysed using RIPA buffer (Sigma) supplemented with 4 mM Na_3VO_4, 50 mM NaF and 1 mM PMSF. Total cell extracts were examined by IP and immunoblot analysis using corresponding antibodies for specific proteins as previously described (Chen and Shively, 2004). IL-1β, IL-6, KC and TNF-α serum amounts were measured with ELISA kits according to manufacturers' manuals (Biolegend and R&D systems).

Supplementary Material

Refer to Web version on PubMed Central for supplementary material.

Acknowledgments

We thank Zuoming Sun for retroviral vectors, Nicole Beauchemin for *Ceacam1*$^{-/-}$ mice and Sofia Loera for histology. This work is supported by NIH grant CA 84202.

References

Avalos BR. Molecular analysis of the granulocyte colony-stimulating factor receptor. Blood. 1996; 88:761–777. [PubMed: 8704229]

Chakraborty A, White SM, Schaefer TS, Ball ED, Dyer KF, Tweardy DJ. Granulocyte colony-stimulating factor activation of Stat3 alpha and Stat3 beta in immature normal and leukemic human myeloid cells. Blood. 1996; 88:2442–2449. [PubMed: 8839834]

Chen CJ, Kirshner J, Sherman MA, Hu W, Nguyen T, Shively JE. Mutation analysis of the short cytoplasmic domain of the cell-cell adhesion molecule CEACAM1 identifies residues that orchestrate actin binding and lumen formation. J Biol Chem. 2007; 282:5749–5760. [PubMed: 17192268]

Chen CJ, Shively JE. The cell-cell adhesion molecule carcinoembryonic antigen-related cellular adhesion molecule 1 inhibits IL-2 production and proliferation in human T cells by association with Src homology protein-1 and down-regulates IL-2 receptor. J Immunol. 2004; 172:3544–3552. [PubMed: 15004155]

Chen Z, Chen L, Qiao SW, Nagaishi T, Blumberg RS. Carcinoembryonic antigen-related cell adhesion molecule 1 inhibits proximal TCR signaling by targeting ZAP-70. J Immunol. 2008; 180:6085–6093. [PubMed: 18424730]

Christopher MJ, Link DC. Regulation of neutrophil homeostasis. Curr Opin Hematol. 2007; 14:3–8. [PubMed: 17133093]

Croker BA, Metcalf D, Robb L, Wei W, Mifsud S, DiRago L, Cluse LA, Sutherland KD, Hartley L, Williams E, et al. SOCS3 is a critical physiological negative regulator of G-CSF signaling and emergency granulopoiesis. Immunity. 2004; 20:153–165. [PubMed: 14975238]

Eash KJ, Means JM, White DW, Link DC. CXCR4 is a key regulator of neutrophil release from the bone marrow under basal and stress granulopoiesis conditions. Blood. 2009; 113:4711–4719. [PubMed: 19264920]

Forlow SB, Schurr JR, Kolls JK, Bagby GJ, Schwarzenberger PO, Ley K. Increased granulopoiesis through interleukin-17 and granulocyte colony-stimulating factor in leukocyte adhesion molecule-deficient mice. Blood. 2001; 98:3309–3314. [PubMed: 11719368]

Gray-Owen SD, Blumberg RS. CEACAM1: contact-dependent control of immunity. Nat Rev Immunol. 2006; 6:433–446. [PubMed: 16724098]

Greten FR, Arkan MC, Bollrath J, Hsu LC, Goode J, Miething C, Goktuna SI, Neuenhahn M, Fierer J, Paxian S, et al. NF-kappaB is a negative regulator of IL-1beta secretion as revealed by genetic and pharmacological inhibition of IKKbeta. Cell. 2007; 130:918–931. [PubMed: 17803913]

Hemmila E, Turbide C, Olson M, Jothy S, Holmes KV, Beauchemin N. Ceacam1a-/- mice are completely resistant to infection by murine coronavirus mouse hepatitis virus A59. J Virol. 2004; 78:10156–10165. [PubMed: 15331748]

Johnnidis JB, Harris MH, Wheeler RT, Stehling-Sun S, Lam MH, Kirak O, Brummelkamp TR, Fleming MD, Camargo FD. Regulation of progenitor cell proliferation and granulocyte function by microRNA-223. Nature. 2008; 451:1125–1129. [PubMed: 18278031]

Kruger J, Butler JR, Cherapanov V, Dong Q, Ginzberg H, Govindarajan A, Grinstein S, Siminovitch KA, Downey GP. Deficiency of Src homology 2-containing phosphatase 1 results in abnormalities in murine neutrophil function: studies in motheaten mice. J Immunol. 2000; 165:5847–5859. [PubMed: 11067945]

Lee CK, Raz R, Gimeno R, Gertner R, Wistinghausen B, Takeshita K, DePinho RA, Levy DE. STAT3 is a negative regulator of granulopoiesis but is not required for G-CSF-dependent differentiation. Immunity. 2002; 17:63–72. [PubMed: 12150892]

Lieschke GJ, Grail D, Hodgson G, Metcalf D, Stanley E, Cheers C, Fowler KJ, Basu S, Zhan YF, Dunn AR. Mice lacking granulocyte colony-stimulating factor have chronic neutropenia, granulocyte and macrophage progenitor cell deficiency, and impaired neutrophil mobilization. Blood. 1994; 84:1737–1746. [PubMed: 7521686]

Liu F, Wu HY, Wesselschmidt R, Kornaga T, Link DC. Impaired production and increased apoptosis of neutrophils in granulocyte colony-stimulating factor receptor-deficient mice. Immunity. 1996; 5:491–501. [PubMed: 8934575]

Lobo EO, Zhang Z, Shively JE. Pivotal advance: CEACAM1 is a negative coreceptor for the B cell receptor and promotes CD19-mediated adhesion of B cells in a PI3K-dependent manner. J Leukoc Biol. 2009; 86:205–218. [PubMed: 19454653]

McLemore ML, Grewal S, Liu F, Archambault A, Poursine-Laurent J, Haug J, Link DC. STAT-3 activation is required for normal G-CSF-dependent proliferation and granulocytic differentiation. Immunity. 2001; 14:193–204. [PubMed: 11239451]

Nagaishi T, Pao L, Lin SH, Iijima H, Kaser A, Qiao SW, Chen Z, Glickman J, Najjar SM, Nakajima A, et al. SHP1 phosphatase-dependent T cell inhibition by CEACAM1 adhesion molecule isoforms. Immunity. 2006; 25:769–781. [PubMed: 17081782]

Nathan C. Neutrophils and immunity: challenges and opportunities. Nat Rev Immunol. 2006; 6:173–182. [PubMed: 16498448]

Roberts AW, Foote S, Alexander WS, Scott C, Robb L, Metcalf D. Genetic influences determining progenitor cell mobilization and leukocytosis induced by granulocyte colony-stimulating factor. Blood. 1997; 89:2736–2744. [PubMed: 9108391]

Singer BB, Klaile E, Scheffrahn I, Muller MM, Kammerer R, Reutter W, Obrink B, Lucka L. CEACAM1 (CD66a) mediates delay of spontaneous and Fas ligand-induced apoptosis in granulocytes. Eur J Immunol. 2005; 35:1949–1959. [PubMed: 15909305]

Singer BB, Scheffrahn I, Heymann R, Sigmundsson K, Kammerer R, Obrink B. Carcinoembryonic antigen-related cell adhesion molecule 1 expression and signaling in human, mouse, and rat leukocytes: evidence for replacement of the short cytoplasmic domain isoform by glycosylphosphatidylinositol-linked proteins in human leukocytes. J Immunol. 2002; 168:5139–5146. [PubMed: 11994468]

Stark MA, Huo Y, Burcin TL, Morris MA, Olson TS, Ley K. Phagocytosis of apoptotic neutrophils regulates granulopoiesis via IL-23 and IL-17. Immunity. 2005; 22:285–294. [PubMed: 15780986]

Tian SS, Lamb P, Seidel HM, Stein RB, Rosen J. Rapid activation of the STAT3 transcription factor by granulocyte colony-stimulating factor. Blood. 1994; 84:1760–1764. [PubMed: 7521688]

Welte T, Zhang SS, Wang T, Zhang Z, Hesslein DG, Yin Z, Kano A, Iwamoto Y, Li E, Craft JE, et al. STAT3 deletion during hematopoiesis causes Crohn's disease-like pathogenesis and lethality: a critical role of STAT3 in innate immunity. Proc Natl Acad Sci U S A. 2003; 100:1879–1884. [PubMed: 12571365]

Yu H, Pardoll D, Jove R. STATs in cancer inflammation and immunity: a leading role for STAT3. Nat Rev Cancer. 2009; 9:798–809. [PubMed: 19851315]

Zhang H, Nguyen-Jackson H, Panopoulos AD, Li HS, Murray PJ, Watowich SS. STAT3 controls myeloid progenitor growth during emergency granulopoiesis. Blood.

Zhu G, Augustine MM, Azuma T, Luo L, Yao S, Anand S, Rietz AC, Huang J, Xu H, Flies AS, et al. B7-H4-deficient mice display augmented neutrophil-mediated innate immunity. Blood. 2009; 113:1759–1767. [PubMed: 19109567]

Abbreviations

CEACAM1	Carcinoembryonic antigen-related cell adhesion molecule 1
ITIM	immunoreceptor tyrosine-based inhibition motif
SHP-1	Src homology 2 (SH2) domain–containing protein-tyrosine phosphatases-1
BM	bone marrow
BMN	bone marrow neutrophil
PB	peripheral blood
PBN	peripheral blood neutrophil
Lin$^-$ BM	lineage negative bone marrow
KC	keratinocyte-derived chemokine
G-CSF	granulocyte-colony stimulating factor
G-CSFR	granulocyte-colony stimulating factor receptor
Stat3	signal transducer and activator of transcription 3
CMP	common myeloid progenitors
GMP	granulocyte-monocyte progenitors
MEP	megakaryocyte erythrocyte progenitors
H&E	hemaotxylin/eosin
LM	*Listeria Monocytogenes*

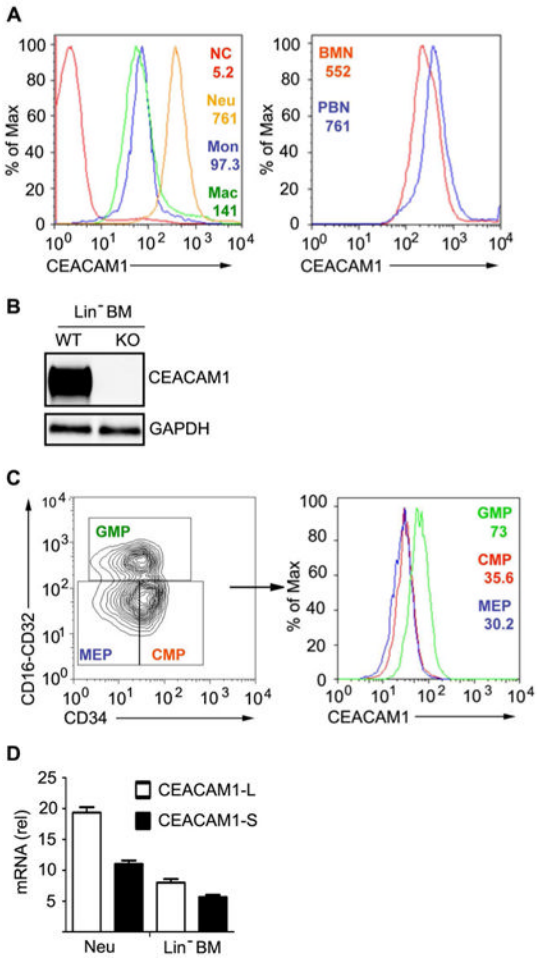

Figure 1. CEACAM1 expression correlates with granulocytic lineage differentiation

A. Quantification of CEACAM1 surface expression amount of PB neutrophils (Ly-6G$^+$CD11b$^+$), monocytes (Ly-6C$^+$CD11b$^+$) and macrophages (Ly-6C$^-$, CD11b$^+$, F4/80$^+$) (left panel, NC, negative control) and a comparison of CEACAM1 expression on BM neutrophils (BMN) and PB neutrophils (PBN) from WT mice (right panel) by flow cytometry shown by mean fluorescence intensity (MFI). **B**. Immunoblot showing the CEACAM1 expression by anti-murine CEACAM1 antibody (CC1) in Lin$^-$ BM cells from WT and *Ceacam1*$^{-/-}$ mice. **C**. Flow cytometric quantification of CEACAM1 expression amounts on GMPs, CMPs and MEPs respectively, gated on the Lin$^-$Sca-1$^-$c-Kit$^+$ fraction in cells. **D**. Q-RT PCR showing the CEACAM1 isoform amounts in neutrophils and Lin$^-$ BM cells (mean ±s.d., n=6). Data are representative of three experiments (**A**-**C**).

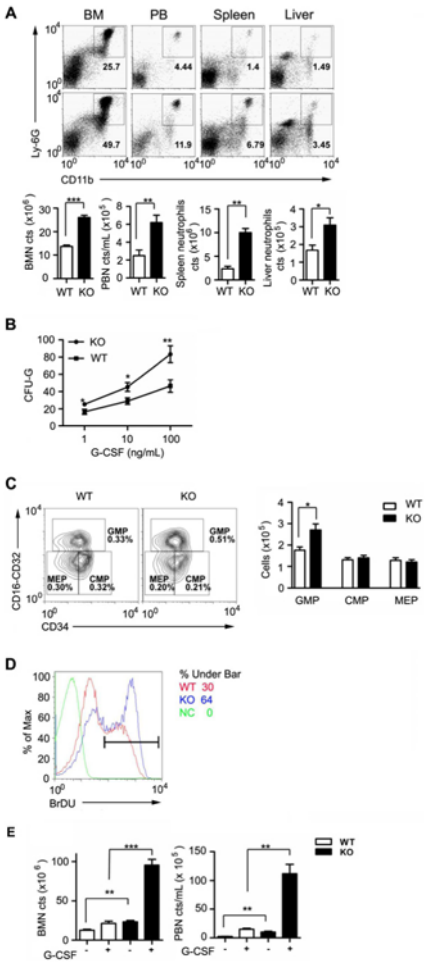

Figure 2. Genetic ablation of CEACAM1 leads to dysregulated granulopoiesis due to neutrophil progenitor cell hyper-proliferation

A. Representative flow cytometric analysis showing Ly-6G$^+$, CD11b$^+$ neutrophil population in BM, spleen, peripheral blood and liver from WT and *Ceacam1*$^{-/-}$ mice (KO). Total neutrophils shown in bar graphs (mean ±s.e.m., n=12 mice). **B**. Methylcellulose colony formation assays of 1 × 10^5 BM cells in response to varied concentrations of G-CSF (mean ±s.e.m., n=6 mice). **C**. Left: flow cytometric analysis of myeloid progenitor cell populations of WT and *Ceacam1*$^{-/-}$ mice (KO). Right: overall number of progenitors per BM sample from one mouse (mean ±s.e.m., n=8 mice). **D**. Flow cytomteric quantification of in vivo BrdU incorporation of GMPs from WT and *Ceacam1*$^{-/-}$ mice 24 hours post BrdU injection (NC, negative control; percentage = BrdU$^+$ populations). **E**. BM neutrophil (BMN) and peripheral blood neutrophil (PBN) numbers in WT and *Ceacam1*$^{-/-}$ mice after G-CSF treatment are represented in graphs (mean ±s.e.m., n=6 mice). *, P <0.05, **, P <0.005, ***, P <0.0001 (two-tailed Student t tests). Data are representative of 3 experiments (**C** and **D**)

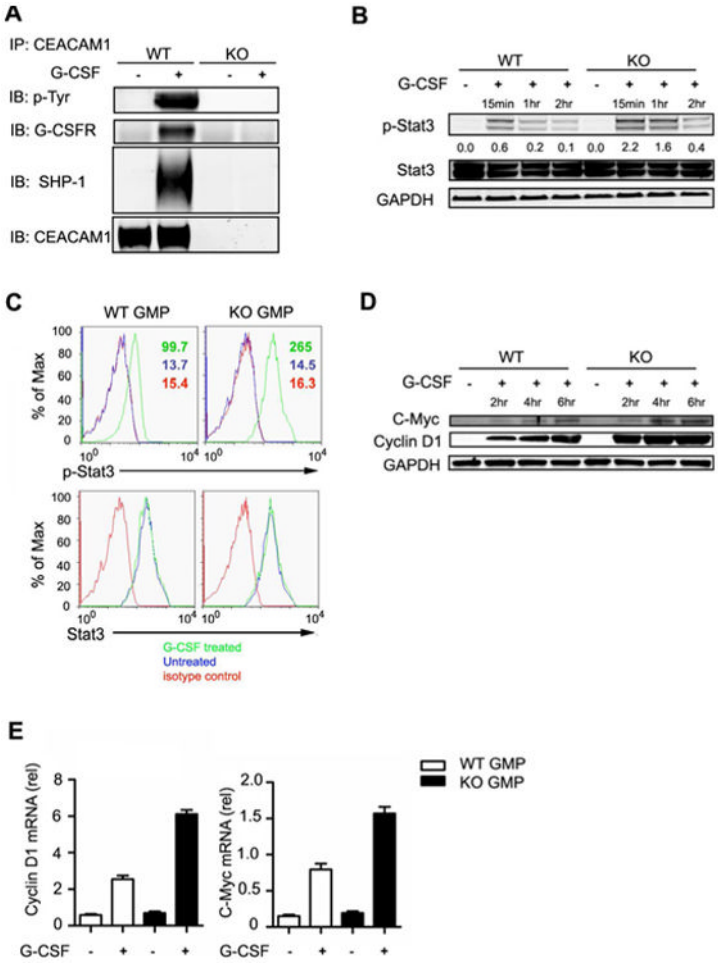

Figure 3. CEACAM1 down-regulates G-CSFR Stat3 signaling

A. Immunoblot analysis of the p-Tyr, G-CSFR, SHP-1 and CEACAM1 in WT and *Ceacam1*$^{-/-}$ (KO) Lin^{-} BM cells with or without G-CSF treatment (40 ng/mL) after IP with CC1 antibody. **B**. Immunoblot analysis of p-Stat3 and Stat3 in WT and *Ceacam1*$^{-/-}$ Lin^{-} BM cells with or without G-CSF treatment (40 ng/mL). Numbers below lanes indicate the ratio of p-Stat3 to GAPDH. **C**. Flow cytometric analysis of intracellular staining of p-Stat3 and Stat3 in WT and KO GMPs with or without G-CSF treatment (40 ng/mL). **D**. Immunoblot analysis of C-Myc and Cyclin D1 in WT and *Ceacam1*$^{-/-}$ Lin^{-} BM cells with or without G-CSF treatment (40ng/ml). **E**. Q-RT PCR showing the Cyclin D1 and C-Myc mRNA amounts in sorted WT and *Ceacam1*$^{-/-}$ GMPs. Data are representative of 3 experiments (**A-E**).

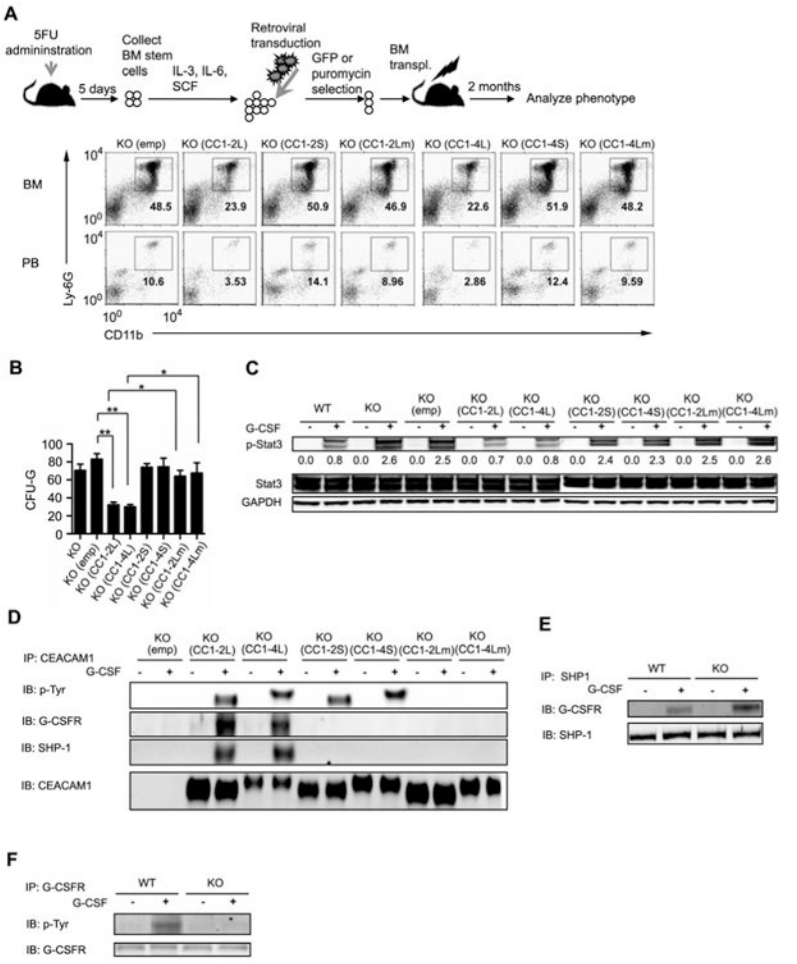

Figure 4. CEACAM1 inhibits G-CSFR-Stat3 signaling and granulopoiesis through ITIM recruitment of SHP-1

A. Experimental design for retroviral transduction and BM reconstitution (top) and representative flow cytometric analysis showing Ly-6G$^+$,CD11b$^+$ neutrophil population in BM and peripheral blood in *Ceacam1*$^{-/-}$ mice (KO) reintroduced with empty vector (emp), CEACAM1-2L (CC1-2L), CEACAM1-4L (CC1-4L), CEACAM1-2S (CC1-2S), CEACAM1-4S (CC1-4S), ITIMs mutated CEACAM1-2L (CC1-2Lm) and ITIMs mutated CEACAM1-4L (CC1-4Lm). **B**. Methylcellulose colony formation assay of 1×10^5 BM cells from *Ceacam1*$^{-/-}$ (KO) with empty vector (emp), CC1-2L, CC1-4L, CC1-2S, CC1-4S, CC1-2Lm and CC1-4Lm chimeras in response to G-CSF (100 ng/mL; mean ±s.e.m., n=6 mice). **C**. Immunoblot analysis of p-Stat3 and Stat3 in *Ceacam1*$^{-/-}$ mice (KO) with empty vector (emp), CC1-2L, CC1-4L, CC1-2S, CC1-4S, CC1-2Lm and CC1-4Lm Lin$^-$ BM cells with or without G-CSF treatment (40 ng/mL). Numbers below lanes indicate ratio of p-Stat3 to GAPDH. **D**. Immunoblot analysis of the p-Tyr, G-CSFR, SHP-1 and CEACAM1 in Ceacam1-/- mice (KO) with empty vector (emp), CC1-2L, CC1-4L, CC1-2S, CC1-4S, CC1-2Lm and CC1-4Lm Lin$^-$ BM cells with or without G-CSF treatment (40 ng/mL) after IP with CC1 antibody. **E**. Immunoblot analysis of G-CSFR and SHP-1 in WT and *Ceacam1*$^{-/-}$ Lin$^-$ BM cells with or without G-CSF treatment (40 ng/mL) after IP with anti-SHP-1. **F**. Immunoblot analysis of p-Tyr and G-CSFR in WT and *Ceacam1*$^{-/-}$ Lin$^-$ BM cells with or without G-CSF treatment (40 ng/mL) after IP with anti-G-CSFR. *, P <0.05, **, P <0.005 (two-tailed Student t-test). Data are representative of 3 experiments (**A, C, D, E** and **F**).

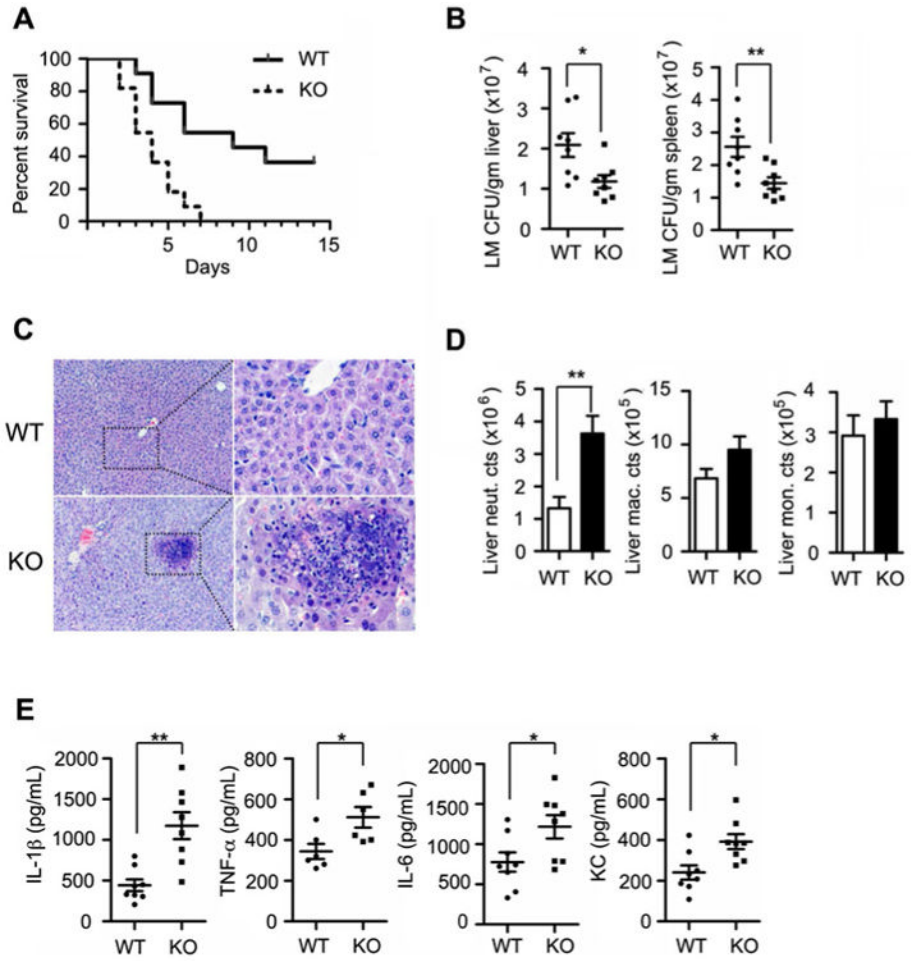

Figure 5. *Ceacam1*$^{-/-}$ mice are hypersensitive to *Listeria Monocytogenes* infection

A. Survival of WT and *Ceacam1*$^{-/-}$ mice (KO) (n=12 per group) after LM infection (i.p. injection of 2.5 × 10^5 CFUs per mouse). **B**. LM colony number in the liver and spleen of WT and *Ceacam1*$^{-/-}$ mice 72 hours post infection (n=8 per group). **C**. H&E staining showing liver sections from WT and *Ceacam1*$^{-/-}$ mice 72 hours post infection. Note the severe tissue damage and necrosis (see high magnification) in the liver from *Ceacam1*$^{-/-}$ mice. **D**. Total number of neutrophils (Ly-6G$^+$,CD11b$^+$), monocytes (Ly-6C$^+$,CD11b$^+$) and macrophages (Ly-6C$^-$,CD11b$^+$,F4/80$^+$) recovered from livers of WT and *Ceacam1*$^{-/-}$ mice 72 hours post infection (mean ±s.e.m., n=8 mice). **E**. Serum amounts of IL-1β, IL-6, TNF-α and KC from WT and *Ceacam1*$^{-/-}$ mice 24 hours after infection (mean ±s.e.m., n=8 mice). *, P <0.05. **, P <0.005 (two-tailed Student t-test).

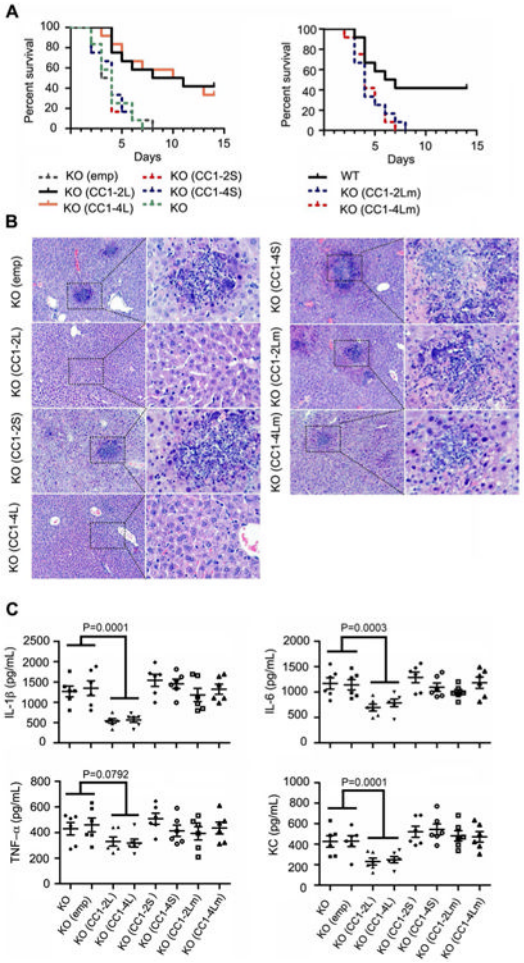

Figure 6. Reintroduction of CEACAM1 long isoforms restores host sensitivity to LM infection

A. Survival of *Ceacam1*$^{-/-}$ mice (KO) with empty vector (emp), CC1-2L, CC1-4L, CC1-2S, CC1-4S, CC1-2Lm and CC1-4Lm chimeras (n=12 per group) after LM infection (i.p. injection of 2.5×10^5 CFUs per mouse). **B**. H&E staining showing liver sections (see high magnification) from *Ceacam1*$^{-/-}$ mice (KO) with empty vector (emp), CC1-2L, CC1-4L, CC1-2S, CC1-4S, CC1-2Lm and CC1-4Lm chimeras 72 hours post infection. **C**. Serum amounts of IL-1β, IL-6, TNF-α and KC from *Ceacam1*$^{-/-}$ mice (KO) with empty vector (emp), CC1-2L, CC1-4L, CC1-2S, CC1-4S, CC1-2Lm and CC1-4Lm chimeras 24 hours after infection (mean ±s.e.m., n=6 mice). P values were calculated between groups indicated by bars using one-way ANOVA.

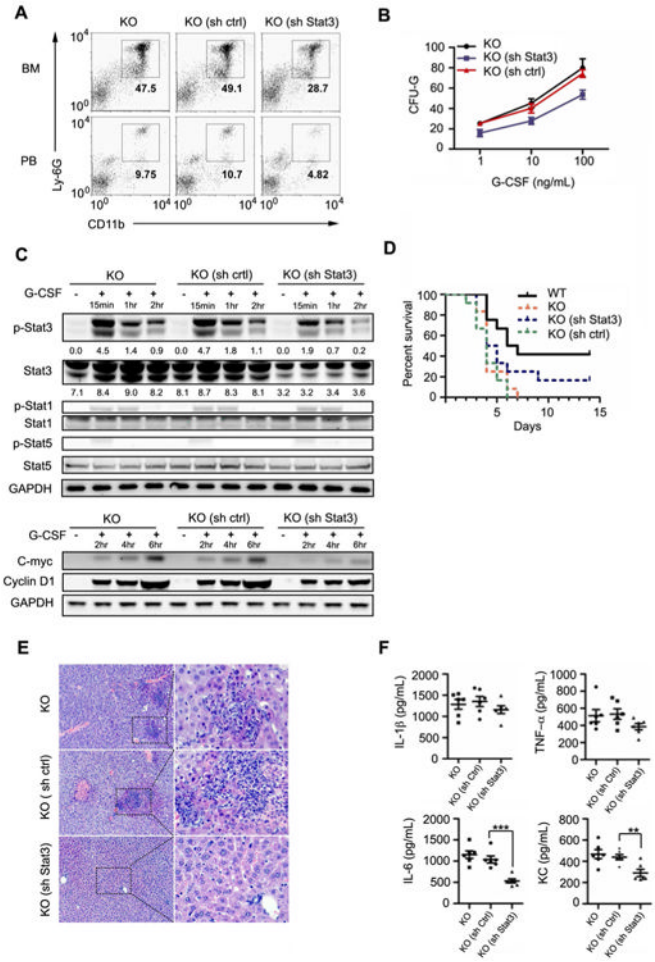

Figure 7. shRNA reduction of Stat3 restores normal granulopoiesis and attenuates host sensitivity to LM infection of *Ceacam1*$^{-/-}$ mice

A. Flow cytomteric analysis of Ly-6G^{+},CD11b^{+} neutrophils in BM and PB in *Ceacam1*$^{-/-}$ mice reconstituted with shRNA control retroviral vector transduced *Ceacam1*$^{-/-}$ (KO) BM cells (sh Ctrl) or sh Stat3 retroviral vector transduced *Ceacam1*$^{-/-}$ (KO) BM cells (sh Stat3) compared with *Ceacam1*$^{-/-}$ BM (KO). **B**. Methylcellulose colony formation assay of 1 × 10^5 BM cells from *Ceacam1*$^{-/-}$ mice (KO) transduced with shRNA control vector (sh Ctrl) or sh Stat3 vector (sh Stat3) in response to varying concentrations of G-CSF (mean ±s.e.m., n=6 mice). **C**. Upper: Immunoblot analysis of p-Stat3, Stat3, p-Stat1, Stat1, p-Stat5 and Stat5 in *Ceacam1*$^{-/-}$ mice (KO) with sh control (sh Ctrl) or sh Stat3 (shStat3) Lin^{-} BM cells with or without G-CSF treatment (40 ng/mL). Numbers below lanes indicate the ratio of p-Stat3 or Stat3 to GAPDH. Lower: Immunoblot analysis of C-Myc and CyclinD1 in *Ceacam1*$^{-/-}$ mice (KO) with sh control (sh Ctrl) or sh Stat3 (sh Stat3) Lin^{-} BM cells with or without G-CSF treatment (40 ng/mL). **D**. Survival of *Ceacam1*$^{-/-}$ mice (KO) with sh control (sh Ctrl) or sh Stat3 (shStat3) Lin^{-} BM cells (n=12 per group) after LM infection (i.p. injection of 2.5 × 10^5 CFUs per mouse). (**E**) H&E staining showing liver sections (tissue damage and necrosis necrosis as shown in high magnification) from *Ceacam1*$^{-/-}$ mice (KO) with sh control (sh Ctrl) or sh Stat3 (shStat3) Lin^{-} BM cells 72 hours post infection. (**F**) ELISA measurement of serum amounts of IL-1β, IL-6, TNF-α and KC from *Ceacam1*$^{-/-}$ mice (KO) with sh control (sh Ctrl) or sh Stat3 (shStat3) Lin^{-} BM cells 24 hours after infection (mean±s.e.m., n=6 mice). *, P <0.05, **, P <0.005, ***, P <0.0001 (two-tailed Student t-test).